The Astrophysical Journal, 831:131 (5pp), 2016 November 10 doi:10.3847/0004-637X/831/2/131
© 2016. The American Astronomical Society. All rights reserved.

DEPENDENCE OF OCCURRENCE RATES OF SOLAR FLARES AND CORONAL MASS EJECTIONS ON THE SOLAR CYCLE PHASE AND THE IMPORTANCE OF LARGE-SCALE CONNECTIVITY

Kangjin Lee[1], Y.-J. Moon[1], and V. M. Nakariakov[1,2]
[1] School of Space Research, Kyung Hee University, Yongin 446-701, Korea
[2] Centre for Fusion, Space & Astrophysics, Physics Department, University of Warwick, Coventry CV4 7AL, UK
Received 2016 May 2; revised 2016 July 21; accepted 2016 July 25; published 2016 November 3

ABSTRACT

We investigate the dependence of the occurrence rates of major solar flares (M- and X-class) and front-side halo coronal mass ejections (FHCMEs), observed from 1996 to 2013, on the solar cycle (SC) phase for six active McIntosh sunspot group classes: Fkc, Ekc, Dkc, Fki, Eki, and Dki. We classify SC phases as follows: (1) ascending phase of SC 23 (1996–1999), (2) maximum phase of SC 23 (2000–2002), (3) descending phase of SC 23 (2003–2008), and (4) ascending phase of SC 24 (2009–2013). We find that the occurrence rates of major flares and FHCMEs during the descending phase are noticeably higher than those during the other phases for most sunspot group classes. For the most active sunspot group class, Fkc, the occurrence rate of FHCMEs during the descending phase of SC 23 is three times as high as that during the ascending phase of SC 23. The potential of each McIntosh sunspot group class to produce major flares or FHCMEs is found to depend on the SC phase. The occurrence rates (R) of major flares and FHCMEs are strongly anti-correlated with the annual average latitude of the sunspot groups (L): $R \sim L^{-2.07}$ for major flares and $R \sim L^{-2.42}$ for FHCMEs. This finding indicates the possible role of large-scale coronal connectivity, e.g., trans-equatorial loops, in powerful energy releases. Interestingly, this relationship is very similar to that between the volumetric coronal heating rate and X-ray loop lengths, indicating common energy release mechanisms.

Key words: Sun: coronal mass ejections (CMEs) – Sun: flares – sunspots

1. INTRODUCTION

It is well known that solar activity, such as solar flares and coronal mass ejections (CMEs), follows a trend of the solar magnetic cycle. For example, the occurrence of CMEs tends to track the solar cycle (SC) phase and amplitude (Webb & Howard 1994). Several studies have shown that the epochs of strong flares or CME activity do not coincide with the maximum phases of SCs (e.g., Svestka 1995; Bai 2006; Hudson et al. 2014). In particular, Svestka (1995) compared the characteristics of solar activity in the descending phases of several SCs and found that the most outstanding solar events occur either a few years before or a few years after the maximum phase. Hudson et al. (2014) studied the variation of flare productivity per given active region (AR) over the interval 1975–2012 using the *Geostationary Operational Environmental Satellites* (*GOES*) and *Reuven Ramaty High Energy Solar Spectroscope Imager* (*RHESSI*) data. They found that the number of major flares per AR was approximately constant during SC 21 and 22 but increased significantly during the descending phase of SC 23 (2004–2005). They did not provide reasonable interpretations of this effect.

One conventional way to forecast solar activity (e.g., solar flares and CMEs) is based on the use of morphological sunspot group classifications (Bornmann & Shaw 1994; Gallagher et al. 2002; Wheatland 2004; Li et al. 2008; Colak & Qahwaji 2009; Lee et al. 2012, 2015; Li & Zhu 2013). A representative morphological sunspot group classification is the McIntosh sunspot group classification (McIntosh 1990). It is characterized by the following morphological features of sunspot groups: the presence or distribution of the penumbra and the length of the sunspot group (Z), symmetry of the principal spot in the sunspot group (p), and compactness of the sunspot group (c). Each AR has its own class, which is determined by the combination of these three morphological components. For the last several decades, the National Oceanic and Atmospheric Administration (NOAA) Space Weather Prediction Center has used the McIntosh sunspot group classification for 24, 48, and 72 hr solar flare probabilistic forecasts (Bloomfield et al. 2012; Crown 2012). This information has been widely utilized by many space weather agencies worldwide. The Big Bear Solar Observatory has also provided daily solar activity reports, which include the daily probability of C-, M-, and X-class flares, based on the McIntosh classification (Gallagher et al. 2002). The Automated Solar Activity Prediction is a probabilistic flare forecasting system developed by Bradford University, which uses *Solar and Heliospheric Observatory* (*SOHO*) / MDI continuum and magnetogram images of sunspot groups and automatically identifies their McIntosh classes (Colak & Qahwaji 2009). The above models are based on the assumption that the potential of groups in each McIntosh sunspot group class to produce a major flare or front-side halo CME (FHCME) is independent of the SC phase. To our knowledge, there has been no systematic study on the SC phase effect on the occurrence rates of flares and CMEs for given McIntosh sunspot group classes.

In this work, we investigate the dependence of the occurrence rates of major solar flares and FHCMEs on the SC phase. This paper is organized as follows: In Section 2, we describe the data and analysis. Results are shown in Section 3. Finally, a brief summary and discussion are presented in Section 4.

2. DATA AND ANALYSIS

In this study, we consider sunspot groups of six McIntosh classes (Fkc, Ekc, Dkc, Fki, Eki, and Dki), which are the most productive ones for both major flares and FHCMEs (see Lee et al. 2012, 2015, who used this classification to forecast soft X-ray flares and FHCMEs). The sunspot group class data of all

ARs are available from the NOAA Solar Region Summary (SRS).[3] The characteristics of each AR in the SRS are compiled from up to six observatories in near-real time. The sunspot group areas are the total corrected areas of a group in millionths of the solar hemisphere. The SRS data are issued at 00:30UT every day.

We consider major X-ray flares (*GOES* M- and X-class) using the data from the National Geophysical Data Center (NGDC),[4] which provides soft X-ray flare information, such as the magnitude, location, and AR number of flares. We could identify the ARs for the individual flares using the AR number from the NGDC flare catalog and NOAA SRS data. We identify FHCMEs in the CME online catalog[5] that provides CME information such as appearance date, time, and angular width (Yashiro et al. 2004; Gopalswamy et al. 2009). CMEs have been observed by the Large Angle and Spectrometric Coronagraph (LASCO) onboard the *SOHO* since 1996 (Brueckner et al. 1995). To identify the source locations of FHCMEs, we compare the CME height-time and *GOES* X-ray profiles from the *SOHO*/LASCO CME catalog. To determine the source location of the FHCMEs, we use the locations of flares occurring within two hours of the CME launch time. In the case of uncertain events, we also examine brightening features from other data, such as *SOHO* / Extreme Ultraviolet Imaging images, *Solar Dynamics Observatory* / Atmospheric Imaging Assembly images, *SOHO*/LASCO-C2/C3, and difference images. A more detailed description of our selection of FHCMEs is given in Lee et al. (2015). CMEs that do not occur in ARs are excluded from this study. In addition, as it is difficult to establish whether there was a CME or not during the data gap, we ignore the data in the data gap periods.

Following the previously developed classification of SC phases (Chowdhury et al. 2013; Pishkalo 2014; Ravindra & Javaraiah 2015), we identify the considered time intervals as follows: (1) the ascending phase of SC 23: 1996–1999; (2) the maximum phase of SC 23: 2000–2002; (3) the descending phase of SC 23: 2003–2008; and (4) the ascending phase of SC 24: 2009–2013. For each phase, we calculate the occurrence rates of major flares and FHCMEs as the number of major flares and FHCMEs produced in a given class of sunspot groups, divided by the number of sunspot groups of this class, and consider their evolution with the SC.

3. RESULTS

3.1. Occurrence Rates of Major Flares and FHCMEs as a Function of the SC Phase

Figure 1 shows the occurrence rates of major flares and FHCMEs as a function of the SC phase for the six considered sunspot group classes. The occurrence rates are determined by the number of major flares ($N_{\rm F}^{\rm ph}$) or FHCMEs ($N_{\rm C}^{\rm ph}$) occurring during the time interval of interest, divided by the sum of the daily numbers of ARs of these six classes ($N_{\rm S}^{\rm ph}$) in this time interval, separately for each sunspot group class. The specific values of these parameters are given in Table 1. In the case of the Fkc, Ekc, Dkc, and Dki sunspot group classes, the occurrence rates of major flares and FHCMEs during the descending phase of SC 23 are evidently higher than those during the other phases. In the case of the Fkc class, in particular, the occurrence rate of major X-ray flares during the descending phase of SC 23 (1.38) is three times as high as that during the ascending phase of SC 23 (0.39). The occurrence rate of FHCMEs during the descending phase of SC 23 (0.27) is two times as high as that during the ascending phase of SC 23 (0.13). This effect is most significant for the most major-flare- and CME-productive sunspot group classes (Fkc, Ekc, and Dkc), which correspond to large, asymmetric, and compact sunspot groups (Lee et al. 2012, 2015). However, even though there are such noticeable differences in occurrence rates, existing forecast models (e.g., Gallagher et al. 2002; Colak & Qahwaji 2009; Falconer et al. 2011; Lee et al. 2012, 2015) do not include this effect.

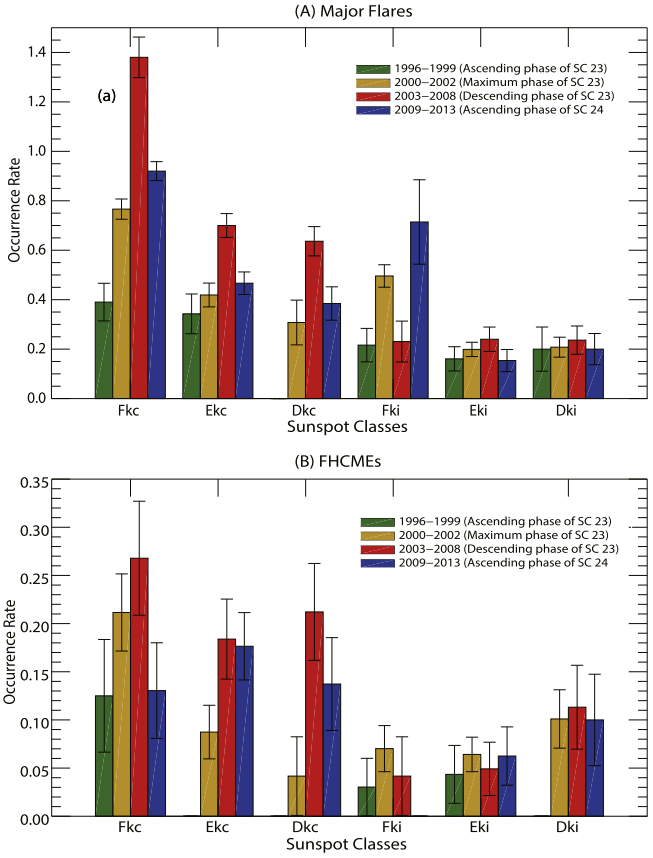

Figure 1. Occurrence rates of major flares ($N_{\rm F}^{\rm ph}/N_{\rm S}^{\rm ph}$) and FHCMEs ($N_{\rm C}^{\rm ph}/N_{\rm S}^{\rm ph}$) for six McIntosh sunspot group classes as a function of the SC phase. Here $N_{\rm F}^{\rm ph}$ is the number of major flares, $N_{\rm C}^{\rm ph}$ is the number of FHCMEs, and $N_{\rm S}^{\rm ph}$ is the sum of the daily numbers of ARs of these six classes in each SC phase. The uncertainty of the occurrence rates (μ) is calculated as $\sigma = \sqrt{\frac{\mu(1-\mu)}{N_{\rm S}^{\rm ann}}}$.

3.2. Annual Occurrence Rates of Major Flares and FHCMEs

Figure 2 shows the occurrence rates of major flares and FHCMEs as a function of year, i.e., the variation of the annual occurrence rates, for all six sunspot group classes combined. The annual occurrence rates are calculated as the total numbers of major flares ($N_{\rm F}^{\rm ann}$) or FHCMEs ($N_{\rm C}^{\rm ann}$) divided by the the sum of the daily numbers of ARs of these six classes ($N_{\rm S}^{\rm ann}$), for a given year. The numbers include sunspot groups of all six considered classes. As shown in the figure, the annual occurrence rates of major flares and FHCMEs during the descending phase are significantly higher than those during the

[3] ftp://ftp.swpc.noaa.gov/pub/warehouse/
[4] www.ngdc.noaa.gov/stp/space-weather/solar-data/solar-features/solar-flares/x-rays/goes/xrs/
[5] http://cdaw.gsfc.nasa.gov/CME_list/

Table 1
Occurrence Rates of Major Flares and FHCMEs

Phase	Fkc	Ekc	Dkc	Fki	Eki	Dki
1996–1999	0.39 (16/41)	0.34 (12/35)	0.00 (0/6)	0.22 (8/37)	0.16 (9/56)	0.20 (4/20)
2000–2002	0.77 (82/107)	0.42 (44/105)	0.31 (8/26)	0.50 (60/121)	0.20 (38/191)	0.21 (21/101)
2003–2008	1.38 (98/71)	0.70 (63/90)	0.64 (42/66)	0.23 (6/26)	0.24 (18/75)	0.24 (13/55)
2009–2013	0.92 (46/50)	0.47 (56/120)	0.38 (20/52)	0.71 (5/7)	0.15 (10/65)	0.20 (8/40)
Phase	Fkc	Ekc	Dkc	Fki	Eki	Dki
1996–1999	0.12 (4/32)	0.00 (0/17)	0.00 (0/4)	0.03 (1/33)	0.04 (2/46)	0.00 (0/11)
2000–2002	0.21 (22/104)	0.09 (9/103)	0.04 (1/24)	0.07 (8/114)	0.06 (12/187)	0.10 (10/99)
2003–2008	0.27 (15/56)	0.18 (16/87)	0.21 (14/66)	0.04 (1/24)	0.05 (3/61)	0.11 (6/53)
2009–2013	0.13 (6/46)	0.18 (21/119)	0.14 (7/51)	0.00 (0/7)	0.06 (4/64)	0.10 (4/40)

Note. The top and bottom tables show the occurrence rates of major flares and FHCMEs, respectively, for six sunspot group classes as a function of the SC phase. The numerator represents the number of major flares or FHCMEs for each phase. The denominator represents the number of ARs for a given sunspot group class for each phase.

other phases, which are different from the trend of monthly sunspot areas. In particular, the annual occurrence rates of both kinds of energy releases have the highest values in 2005.

3.3. Occurrence Rates of Major Flares and FHCMEs as a Function of the Annual Average Latitude of Sunspot Groups

In general, during the initial phase of a SC, sunspots appear at mid-latitude. Then, with the development of the SC, the location of the consecutively appearing sunspots moves toward the equator, a phenomenon illustrated by the butterfly diagram. Thus, the occurrence rates of major solar energy releases may show some scaling with the annual average latitude of sunspots, L. Let us define occurrence rate as the event number per time interval, divided by the number of ARs during this time interval, denoting it $R_{\mathrm{F,C}}$, where the indices correspond to major flares and FHCMEs, respectively. Let us look for the dependence of the occurrence rates $R_{\mathrm{F,C}}$ on L in the form

$$R_{\mathrm{F,C}} \propto L^{\alpha}, \tag{1}$$

where α is a constant exponent.

Figure 3 shows the relationship between the occurrence rates of major flares and FHCMEs and the annual average latitude of sunspot groups of all the six classes under consideration. We approximate the log–log dependences by linear functions. There is a strong anti-correlation between these parameters. Both correlation coefficients in the logarithm are −0.91 for major flares and FHCMEs. We find that the major flare and FHCME occurrence rates scale according to the latitude to the power of

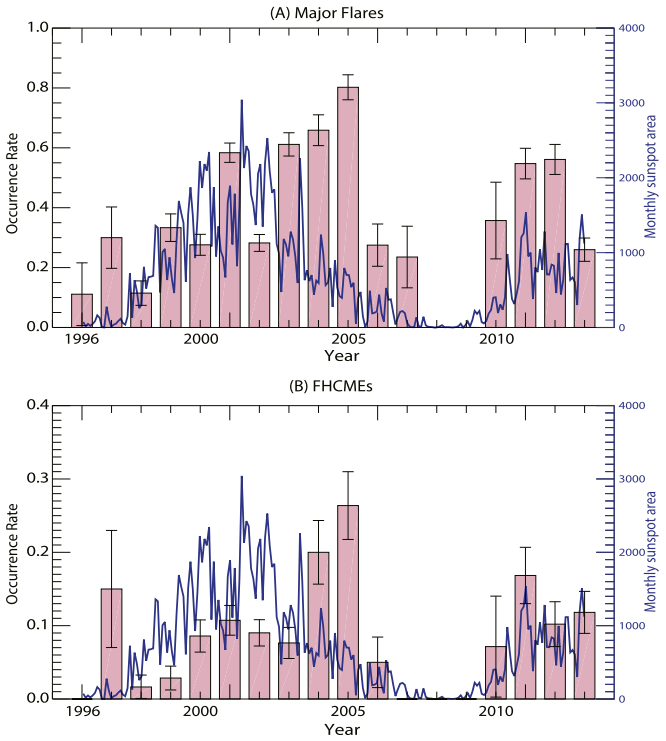

Figure 2. Occurrence rates of major flares ($N_{\mathrm{F}}^{\mathrm{ann}}/N_{\mathrm{S}}^{\mathrm{ann}}$) and FHCMEs ($N_{\mathrm{C}}^{\mathrm{ann}}/N_{\mathrm{S}}^{\mathrm{ann}}$) as a function of year. The solid blue line shows the monthly sunspot area from 1996 to 2013. The uncertainty of the occurrence rates (μ) is calculated as $\sigma = \sqrt{\frac{\mu(1-\mu)}{N_{\mathrm{S}}^{\mathrm{ann}}}}$, where $N_{\mathrm{S}}^{\mathrm{ann}}$ is the sum of the daily numbers of ARs of these six classes in a given year.

$\alpha = 2.07$ and 2.42, respectively. The uncertainties are calculated by the root mean square errors. We do not consider the data of the second ascending period (2009–2013) for the linear fit line because each SC could have different characteristics.

4. SUMMARY AND DISCUSSION

In this study, we investigate the dependence of the occurrence rates of major flares and FHCMEs, observed in the time interval from 1996 to 2013, on the SC phase for six active McIntosh sunspot group classes: Fkc, Ekc, Dkc, Fki, Eki, and Dki. This time interval includes four SC phases: the ascending, maximum, and descending phases of SC 23 and the ascending phase of SC 24.

The main results of this study are summarized as follows. First, for the most major-flare- and FHCME-productive sunspot group classes (Fkc and Ekc), which are characterized by large, asymmetric, and compact sunspot groups, the occurrence rates of major flares and FHCMEs during the descending phase of SC 23 are higher than those during the other phases. In particular, the occurrence rate of FHCMEs during the descending phase of SC 23 for the most active sunspot group class, Fkc, is found to be three times as high as that during the ascending phase of SC 23. Second, the annual occurrence rates of major flares and FHCMEs are the highest in 2005. Third, the occurrence rates of major flares and FHCMEs are strongly anti-correlated with the annual average sunspot group latitude. Our results support the assumption made in previous studies (Bornmann & Shaw 1994; Gallagher et al. 2002; Wheatland 2004; Li et al. 2008; Colak & Qahwaji 2009; Lee et al. 2012, 2015; Li & Zhu 2013) that the potential of groups in each McIntosh sunspot group class to

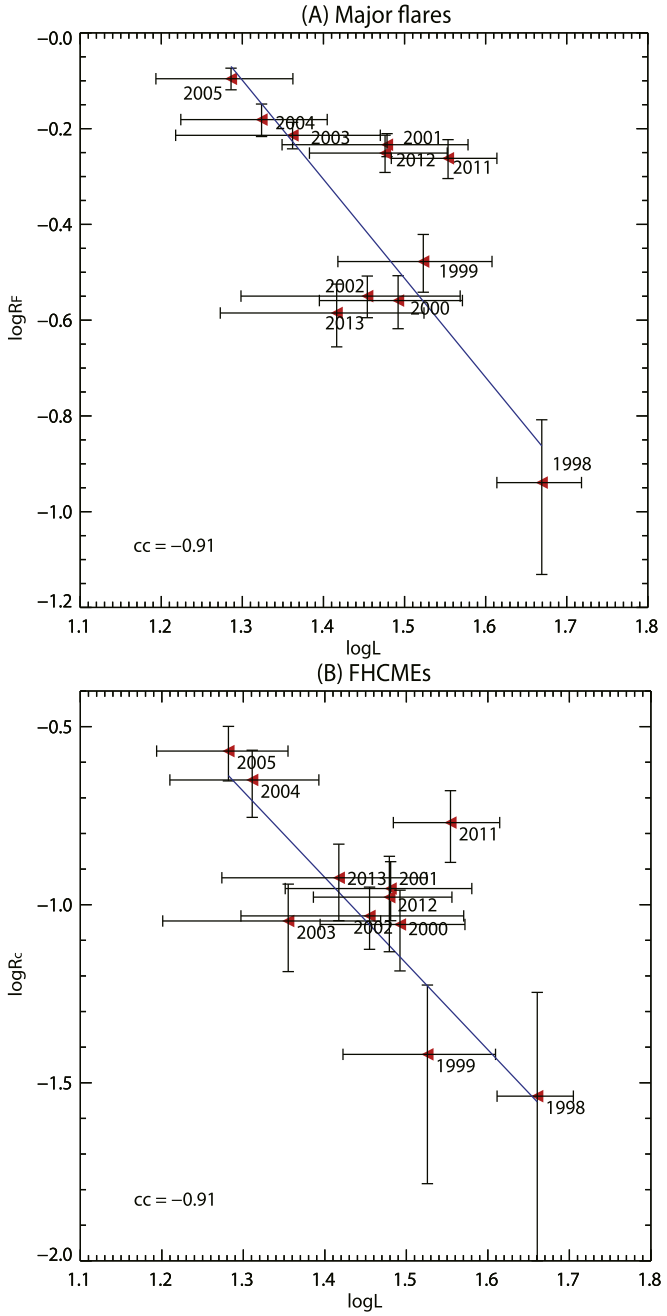

Figure 3. Occurrence rates ($R_{F,C}$) of major flares and FHCMEs as a function of the annual average latitude (L) of the sunspot groups. The red triangles are the occurrence rates of the flares and CMEs. The solid blue line is a linear fitting line in the log–log plot neglecting the data in the second ascending phase (2009–2013). The error bars are calculated by the rms errors. Years with the number of ARs below ten (i.e., 1996, 1997, 2006, 2007, 2008, 2009, and 2010) are excluded.

produce a major flare or FHCME is independent of the SC phase. Our results indicate that the smaller the annual latitude, the higher the expected occurrence rates of major flares and FHCMEs. This effect should be taken into account in the development of forecast models of solar flares and CMEs.

The established increase in the occurrence rates of major flares in the descending phase of the SC in comparison with those in other phases is consistent with previously published findings (e.g., Aschwanden 1994; Svestka 1995; Bai 2006; Yang et al. 2014). We also find that the FHCME occurrence rates have a similar tendency. The established increase in occurrence rates demonstrates that this effect is not a simple reflection of the increase in surface magnetic flux and that the probability of an AR producing a major flare or a CME is controlled by an additional factor that varies with the SC, even for ARs of the same McIntosh class. Therefore, we note that the effect of the SC phase has to be considered when solar flare or CME forecast models are developed.

To explain the variation of the flare occurrence rate with the SC, several possibilities have been proposed (Bai 2006; Chen et al. 2011; Le et al. 2014; McIntosh & Leamon 2014). In particular, Bai (2006) and Le et al. (2014) suggested that the high flaring activity during the descending phase of SC 23 could be associated with the occurrence of super ARs. However, Chen et al. (2011) showed that the number of super ARs is not dominant in the descending phase of SC 23 in the time interval of SC 19–23. McIntosh & Leamon (2014) linked this period of enhanced activity with the latitudinal–temporal interaction of toroidal magnetic flux systems. They found that the number of delta-spot ARs appears to be weighted during the descending phase of SC 23. They deduced that these delta-spot regions form as a consequence of intra- and extra-hemispheric activity band interaction, which results from the mixing polarity of ARs.

The relationship established in our study between the occurrence rates of major flares and FHCMEs and the annual average latitude of sunspot groups may indicate the role of long-distance magnetic connectivity in the dependence of occurrence rates on the SC phase. In particular, the annual average latitude of sunspot groups determines the average length of trans-equatorial loops (TLs). A TL is a coronal loop connecting two separate ARs located in the opposite hemispheres (e.g., Tsuneta 1996; Pevtsov 2000). It has been found to be a common phenomenon, with up to one-third of all ARs exhibiting TLs in soft X-ray images (Pevtsov 2000). Therefore, our results may be a statistical indication that large-scale magnetic connectivities highlighted by TLs are important for producing solar activity such as major flares and FHCMEs. There have been many studies on the topology of the large-scale solar magnetic field structure (e.g., Babcock 1961; Hansen & Hansen 1975) and the relationship between the occurrence of solar flares / CMEs and large-scale magnetic connectivity (e.g., Antiochos et al. 1999; Khan & Hudson 2000; Wang & Sheeley 2003; Wang et al. 2007; Zhou et al. 2007; Fu & Welsch 2016). In particular, Dalla et al. (2007) established that the flaring rate (weakly) increases with the appearance of a new AR within 12° of the pre-existing flaring AR. Also, it has been reported that the interaction of ARs increases as sunspots move toward the equator (McIntosh & Leamon 2014; McIntosh et al. 2014). Such interactions may be related to the reconnection of magnetic fields that belong to different ARs, and the subsequent formation of large-scale structures such as TLs, which play an important role in triggering flares and CMEs (Khan & Hudson 2000). Moon et al. (2002) showed that sympathetic flares are more frequent in TLs than in loops connecting two ARs in the same hemisphere. Chen et al. (2006) examined the relation between the number of soft X-ray TLs and that of ARs each year from 1991 to 2001. They found good correlations of the TL numbers with SC indices, with the increase in TL number during the descending phase of SC 22 in comparison to other phases of SC 22. The effect of the dependence of flaring activity on AR separation and

connectivity may be understood in terms of the interaction of magnetic energy between these ARs (Fu & Welsch 2016).

Interestingly, we obtain the relationship between the occurrence rates of major flares/FHCMEs and the annual average latitude, $R_F \sim L^{-2.07}$ for major flares and $R_C \sim L^{-2.42}$ for FHCMEs. There are many relationships in solar physics and elsewhere that have power-law fittings with indices of -2. In particular, several studies have attempted to determine whether the frequency distribution of microflares and other small-scale solar brightening is the same as that of solar flares (e.g., Aschwanden & Charbonneau 2002; Li et al. 2012). Klimchuk & Porter (1995) and Porter & Klimchuk (1995) determined the dependence of the volumetric coronal heating rate Q on the soft X-ray loop lengths, $Q \propto L^{\alpha}$, with a most probable value of α of -1.95 and a 90% confidence interval of $-3.11 \leqslant \alpha \leqslant -0.95$. This scaling was found to be consistent with the nanoflare heating model by Parker (1983, 1988). A series of follow-up studies demonstrated that the scaling exponent is in the range of -3.11 and -1 (e.g., Mandrini et al. 2000; Warren & Winebarger 2006; Gontikakis et al. 2008; Lundquist et al. 2008). All those studies addressed non-flaring loops. However, considering that non-flaring heating is caused by small-scale flaring events, and assuming a power-law energy distribution of the flare frequency, we deduce that the occurrence rate of flares should have similar $\propto L^{\alpha}$ scaling with the magnetic field line length. This scaling is found in our study. Thus, the consistency between the results we obtain for major flares and those of previous studies of small-scale coronal heating may imply the universality of the energy release mechanism from small-scale to large-scale magnetic reconnection. Furthermore, this relationship may imply that large-scale magnetic reconnections via TLs are important for producing major flares and FHCMEs, especially during the descending phase of SCs.

The authors thank Dr Partha Chowdhury, Eo-Jin Lee, and Harim Lee for their insightful discussions. This work was supported by the BK21 plus program through the National Research Foundation (NRF) funded by the Ministry of Education of Korea, the National Radio Research Agency/Korean Space Weather Center, Basic Science Research Program through the NRF funded by the Ministry of Education (NRF-2016R1A2B4013131) and NRF of Korea Grant funded by the Korean Government (NRF-2013M1A3A3A02042232B4013131). The CME catalog is generated and maintained at the CDAW Data Center by NASA and the Catholic University of America in cooperation with the Naval Research Laboratory. *SOHO* is a project of international cooperation between the ESA and NASA.

REFERENCES

Antiochos, S. K., DeVore, C. R., & Klimchuk, J. A. 1999, ApJ, 510, 485
Aschwanden, M. J. 1994, SoPh, 152, 53
Aschwanden, M. J., & Charbonneau, P. 2002, ApJL, 566, L59
Babcock, H. W. 1961, ApJ, 133, 572
Bai, T. 2006, SoPh, 234, 409
Bloomfield, D. S., Higgins, P., Mcateer, R. T. J., & Gallagher, P. T. 2012, ApJL, 747, L41
Bornmann, P. L., & Shaw, D. 1994, SoPh, 150, 127
Brueckner, G. E., Howard, R. A., & Koomen, M. J. 1995, SoPh, 162, 357
Chen, A. Q., Wang, J. X., Li, J. W., Feynman, J., & Zhang, J. 2011, A&A, 534, A47
Chen, J., Bao, S., & Zhang, H. 2006, SoPh, 235, 281
Chowdhury, P., Choudhary, D. P., & Gosain, S. 2013, ApJ, 768, 188
Colak, T., & Qahwaji, R. 2009, SpWea, 7, S06001
Crown, M. D. 2012, SpWea, 10, S06006
Dalla, S., Fletcher, L., & Walton, N. A. 2007, A&A, 468, 1103
Falconer, D., Barghouty, A. F., Khazanov, I., & Moore, R. 2011, SpWea, 9, S04003
Fu, Y., & Welsch, B. T. 2016, SoPh, 291, 383
Gallagher, P. T., Moon, Y.-J., & Wang, H. 2002, SoPh, 209, 171
Gontikakis, C., Contopoulos, I., & Dara, H. C. 2008, A&A, 489, 441
Gopalswamy, N., Yashiro, S., Michalek, G., et al. 2009, EM&P, 104, 295
Hansen, S. F., & Hansen, R. T. 1975, SoPh, 44, 503
Hudson, H., Fletcher, L., & McTiernan, J. 2014, SoPh, 289, 1341
Khan, J. I., & Hudson, H. S. 2000, GeoRL, 27, 1083
Klimchuk, J. A., & Porter, L. J. 1995, Natur, 377, 131
Le, G., Yang, X., Liu, Y., et al. 2014, Ap&SS, 350, 443
Lee, K., Moon, Y.-J., & Lee, J.-Y. 2015, SoPh, 290, 1661
Lee, K., Moon, Y.-J., Lee, J.-Y., Lee, K.-S., & Na, H. 2012, SoPh, 281, 639
Li, R., Cui, Y., He, H., & Wang, H. 2008, AdSpR, 42, 1469
Li, R., & Zhu, J. 2013, RAA, 13, 1118
Li, Y. P., Gan, W. Q., & Feng, L. 2012, ApJ, 747, 133
Lundquist, L. L., Fisher, G. H., Metcalf, T. R., Leka, K. D., & McTiernan, J. M. 2008, ApJ, 689, 1388
Mandrini, C. H., Demoulin, P., & Klimchuk, J. A. 2000, ApJ, 530, 999
McIntosh, P. S. 1990, SoPh, 125, 251
McIntosh, S. W., & Leamon, R. J. 2014, ApJL, 796, L19
McIntosh, S. W., Wang, X., Leamon, R. J., et al. 2014, ApJ, 792, 12
Moon, Y.-J., Choe, G. S., Park, Y.-D., et al. 2002, ApJ, 574, 434
Parker, E. N. 1983, ApJ, 264, 642
Parker, E. N. 1988, ApJ, 330, 474
Pevtsov, A. 2000, ApJ, 531, 553
Pishkalo, M. I. 2014, SoPh, 289, 1815
Porter, L. J., & Klimchuk, J. A. 1995, ApJ, 454, 499
Ravindra, B., & Javaraiah, J. 2015, NewA, 39, 55
Svestka, Z. 1995, AdSpR, 16, 27
Tsuneta, S. 1996, ApJL, 456, L63
Wang, J., Zhang, Y., Zhou, G., et al. 2007, SoPh, 244, 75
Wang, Y. M., & Sheeley, N. R. 2003, ApJ, 599, 1404
Warren, H. P., & Winebarger, A. R. 2006, ApJ, 645, 711
Webb, D. F., & Howard, R. A. 1994, JGR, 99, 4201
Wheatland, M. S. 2004, ApJ, 609, 1134
Yang, X.-X., Le, G.-M., Zhang, C.-Y., Yin, Z.-Q., & Zhao, W. 2014, ChA&A, 38, 92
Yashiro, S., Gopalswamy, N., Michalek, G., et al. 2004, JGRA, 109, 7105
Zhou, G., Wang, J., Wang, Y., & Zhang, Y. 2007, SoPh, 244, 13